

We are IntechOpen, the world's leading publisher of Open Access books Built by scientists, for scientists

6,900

Open access books available

185,000

International authors and editors

200M

Downloads

Our authors are among the

154

Countries delivered to

TOP 1%

most cited scientists

12.2%

Contributors from top 500 universities



WEB OF SCIENCE™

Selection of our books indexed in the Book Citation Index
in Web of Science™ Core Collection (BKCI)

Interested in publishing with us?
Contact book.department@intechopen.com

Numbers displayed above are based on latest data collected.
For more information visit www.intechopen.com



Identification and Quantification of Phases in Steels by X Ray Diffraction Using Rietveld Refinement

Adriana da Cunha Rocha and Gabriela Ribeiro Pereira

Abstract

X-ray diffraction has been applied in the investigation of phase formation in steels, operating in industrial environments. In this work, identification and quantification of phases by X-ray diffraction and peak fitting, using the Rietveld method, were employed. In a first scenario, two different types of steels, subjected to abrasive surface cleaning, suffered contamination from the blasting operation that compromise between 10 and 36% of the blasted surface, as revealed by the quantitative phase analysis. Such high values of particulates can jeopardize the corrosion protection offered by posterior coating application. In a second scenario, duplex steels (DS) subjected to aggressive environments and high temperatures of service went through phase transformation that formed amounts up to 3.5% of a deleterious phase, known as sigma phase. This phase compromises the steel mechanical resistance and corrosion protection, and its quantification is crucial for the assurance of the material integrity. The quantitative phase analysis (QPA) by X-ray diffraction provided the diagnosis of forthcoming problems related to the presence of such phases in the investigated steels, allowing the optimization of techniques and the choice of correct process parameters.

Keywords: X-ray diffraction, steels, Rietveld refinement, phase quantification

1. Introduction

Steel is the most common material used on earth. Applications vary from simple cutlery to spacecraft parts and are so vast; one finds even hard to list it all. This is mainly due to the versatility found in this type of iron and carbon alloy, in terms of physical, mechanical, and chemical properties. Also, when compared to other types of materials, steels are economically affordable. Therefore, steel has been studied for many decades and will continue to be so in the forthcoming years. Industrial plants have most of their equipment made of steel. Applications involving the oil and gas industry are very demanding in terms of optimizing the use of these steels for high performance in constant aggressive environments. In this case, the ultimate need is for steels that can resist both heavy loads and aggressive corrosive environments.

Some new classes of steels, such as the duplex steels, are of very much of interest nowadays, because of their good compromise between mechanical resistance and

corrosion protection [1, 2]. As any other metallic material though, they usually need thermal-mechanical processing in order to be adequate to the different uses. Thermal-activated processes may lead to the creation of new phases in the steel—some intentionally promoted, but some not. The knowledge of phase transformations in steels is mandatory to forecast the properties the material will acquire after such transformations [3]. Because steel has a long of range periodic atomic structure, with well-defined crystallographic aspects [4], X-ray diffraction [5] is one of the most important analytical techniques to identify those structures, in order to understand steel properties.

Lately, the identification and quantification of phases have been upgraded by many methods of peak refinement. These methods provide a good calculation of crystallographic parameters, enabling precise measurements to be performed in different materials. Among those methods, the Rietveld refinement [6] has been gaining space among crystallographers due to its analytical capabilities. A general overview of the Rietveld profile fitting and quantitative phase analysis is provided in the following sections. Then, two specific applications of X-ray diffraction for steel phase analysis are described. The first case refers to the quantification of contaminants on steel substrates after jet impingement, aiming corrosion resistance by organic coatings. The second case is related to the phase transformations occurring in a type of steel used in oil and gas applications, when this material is subjected to high temperatures due to welding procedures or operation in service. In both situations, peak refinement is made, for the calculation of crystallographic parameters and for quantitative phase calculations.

2. Peak refinement and quantitative phase analysis: the Rietveld method

X-ray profile fitting provides important crystallographic information from the analyzed material. There are several different techniques nowadays, but one of them, known as the Rietveld refinement method, has many advantages over the others. In this method, first presented by Hugo Rietveld to refine nuclear and magnetic structures [6] and lately developed by many scientists [7], least-squares refinements are carried out until the best fit is obtained between the entire observed powder diffraction pattern and the full calculated pattern. The quantity minimized in the least-squares refinement is the residual S_y :

$$S_y = \sum_i w_i (y_i - y_{ci})^2 \quad (1)$$

where y_i = observed intensity at the i -th step; y_{ci} = calculated intensity at the i -th step; $w_i = 1/y_i$.

The equation model applied for the method (Eq. 2) considers the following parameters:

- The Bragg reflections contributing to a specific intensity y_i at every specific i point in the whole pattern
- A scale factor s
- The Miller indices, h, k, l , for a Bragg reflection, represented by K
- The Lorentz polarization and multiplication factors L_K
- The reflection profile function \varnothing

- The preferred orientation function P_k
- The absorption factor A
- The structure factor modulus for the k^{th} Bragg reflection $|F_k|$
- The background intensity at the i -th step, y_{bi}

$$y_{ci} = s \sum_K L_K |F_K|^2 \delta(2\theta_i - 2\theta_k) P_K A + y_{bi} \quad (2)$$

Quantitative phase analysis using the Rietveld method [8] employs the relative weight fraction W of each phase p in a mixture of n phases calculated according to the equation:

$$W_p = (s_p ZMV) / \sum_{i=1}^n s_i (ZMV)_i \quad (3)$$

where s is the Rietveld scale factor, Z is number of formula units per unit cell, M is the mass of the formula unit (atomic mass unit), and V is the unit cell volume (\AA^3).

The following sections will present two specific cases of the utilization of the Rietveld refinement method with further quantitative phase analysis (QPA). Those practical cases demonstrate how this methodology was applied for the analysis of steel parts, addressing the presence of unwanted phases and phase unbalance due to thermal treatments performed in specific steels.

3. Case 1: abrasive blasting in steel surfaces—addressing contamination by X-ray diffraction quantitative analysis

Duplex and super duplex steels (DS and SDS, respectively) have been widely used in oil and gas industries because of their advantages over other steel types in terms of mechanical properties and corrosion resistance [1, 2]. The harsh environments where those steels are in service require protection from degradation that can be found in organic coatings [9, 10].

The coating performance is highly dependent on the surface pretreatment and the application procedures [11, 12]. Those must be in accordance with standard documents [13, 14], which include procedures for blast cleaning. Blasting processes though might affect the coating adhesion and corrosion rate, depending on the degree of contamination from the abrasive particulate material used, as those particulates can promote local pH changes and/or galvanic effects [15]. The common abrasives employed for surface treatment of steels are aluminum oxide and martensitic steel abrasives due to their high values of hardness. Pulverization of the grits, however, can lead to undesired particulate depositions over the steel surfaces (**Figure 1**), which induce local alkalization, decreasing the protection. Because of all these factors, substrate contamination needs to be engaged in an efficient fashion, to avoid damages on the performance of the whole system.

Determination of the inclusion or second-phase constituent, by metallographic analysis [16], can be used to account for such contamination. However, the technique can be quite time-consuming. Quantitative phase analysis by X-ray diffraction though can be used for such task [17–22]. The Rietveld method can provide very accurate estimative of the relative and/or absolute amount of the component phases [22–25] and has advantages over traditional internal-standard-based

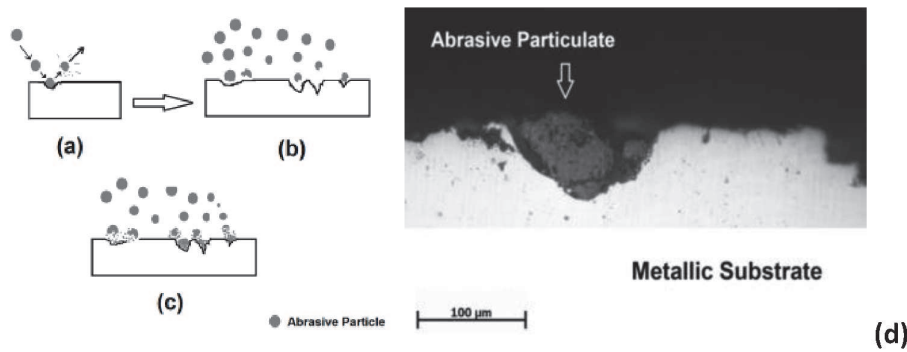


Figure 1. (a, b) Abrasive particles hitting a metal substrate surface and (c) abrasive fragments deposited over the surface. (d) A real micrographs of a particulate allocated in the valley created by the particle impact in the surface.

techniques. Surface roughness effects can also be considered and compensated by correction functions, which makes the Rietveld method more interesting to this type of process.

3.1 Surface roughness corrections

In Rietveld analysis of X-ray powder diffraction patterns, the effect of surface roughness (SR) of absorbing polycrystalline samples can be a source of systematic errors [26–30]. The SR effect can reduce the intensity of low-angle reflections and lead to anomalous low values of refined atomic displacement parameters. Depending on the degree of SR, the isotropic atom displacement can lead to negative values, which have no physical meaning. To correct such effects, a SR Suortti Model [31] has been used to guarantee a higher flexibility in terms of angular ranges.

3.2 Experimental parameters

ASTM A516 G60 carbon steel (CS) and UNS 32760 super duplex steel (SDS) samples were used as metallic substrates subjected to the blasting process. The abrasives used encompassed two types of aluminum oxide particulate (sintered bauxite (SB) and demagnetized alumina (DA)). A D8 Discover Bruker AXS was the equipment used for data acquisition. The diffraction parameters are listed as following:

- Radiation: Co K α ($\lambda = 1789 \text{ \AA}$).
- Current and voltage: 40 mA 35 kV.
- Primary optics: Co Göbel Mirror, two slits of 1 mm and 6 mm and a soller slit with 2 cm x 1 cm aperture.
- Secondary optics: K β filter, 8 mm slit, axial soller slit with divergence of 2.5°.
- Detector: point scanning detector—PSD type.
- 2θ range = 10° to 110°.
- Step-size: 0.001°.
- Scanning velocity was 0.5 s/step.

Rietveld analysis was carried out using Diffrac PlusTOPAS (ver 4.2) software [32, 33].

3.3 X-ray analysis results

Diffraction patterns were obtained for both substrate bulks, prior to the blasting process, to work as a reference pattern when measuring the degree of contamination of the samples subsequently analyzed. In the blasted surfaces, α -Fe (ferrite) [34] was observed in CS substrate, while α -Fe and γ -Fe [35] (ferrite and austenite, respectively) were present in the SDS substrate.

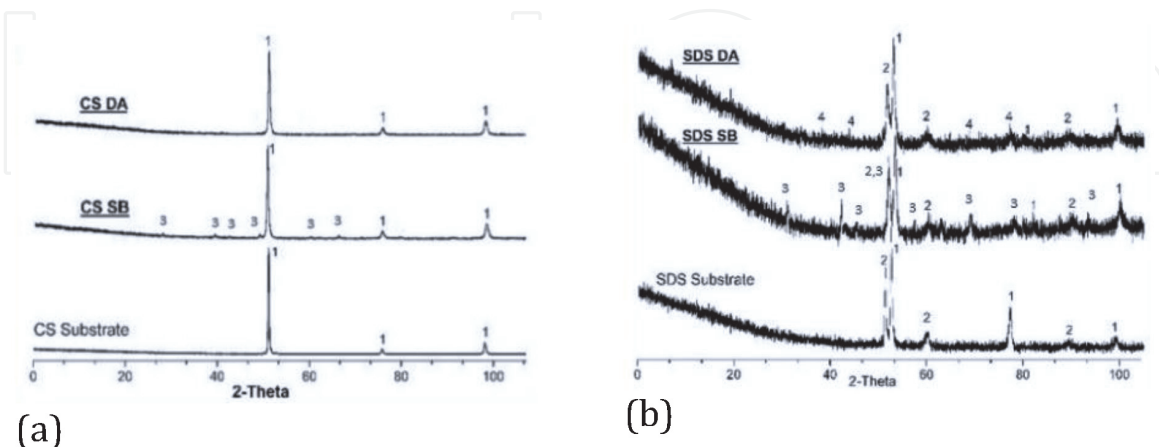
The commercial SB abrasive showed a predominance of phase alpha alumina (α -Al₂O₃) [36] which was verified in the SB abrasive, while the DA abrasive presented a majority of kappa alumina (κ -Al₂O₃) [37]. **Figure 2** presents the diffraction patterns for the carbon steel substrate before and after abrasive blasting (a) and for the super duplex steel before and after blasting (b), respectively.

Figure 3 shows the detailed refined scan for the carbon steel substrate blasted with κ -Al₂O₃ from the DA abrasive and α -Al₂O₃ originated from the SB abrasive. In the same manner, **Figure 4** presents the result of the refined scan from the SDS substrate blasted with κ -Al₂O₃ from the DA abrasive and α -Al₂O₃ originated from the SB abrasive.

3.3.1 Fitting parameters

The structure refinement functions and parameters are listed as following:

- Chebyshev polynomial of fourth degree [38] and Topas 1/x background function and (background fitting intensities, y_{ib})
- Preferred orientation (PO) March-Dollase model [39–41] for calculating the preferred crystal orientations of α -Fe and γ -Fe phases (this is mandatory especially for processed steel products like ingots, sheets, and pipe sections)
- PO spherical harmonics [42] model of order 6 for the alumina phase



Number	1	2	3	4
Phase	Fe- α	Fe- γ	α -Al ₂ O ₃	κ -Al ₂ O ₃

Figure 2. (a) CS substrate after DA and SB blasting and (b) SDS substrate after DA and SB blasting. When blasting is performed with Al₂O₃ abrasives, one can see contamination by the new peaks introduced to the scans.

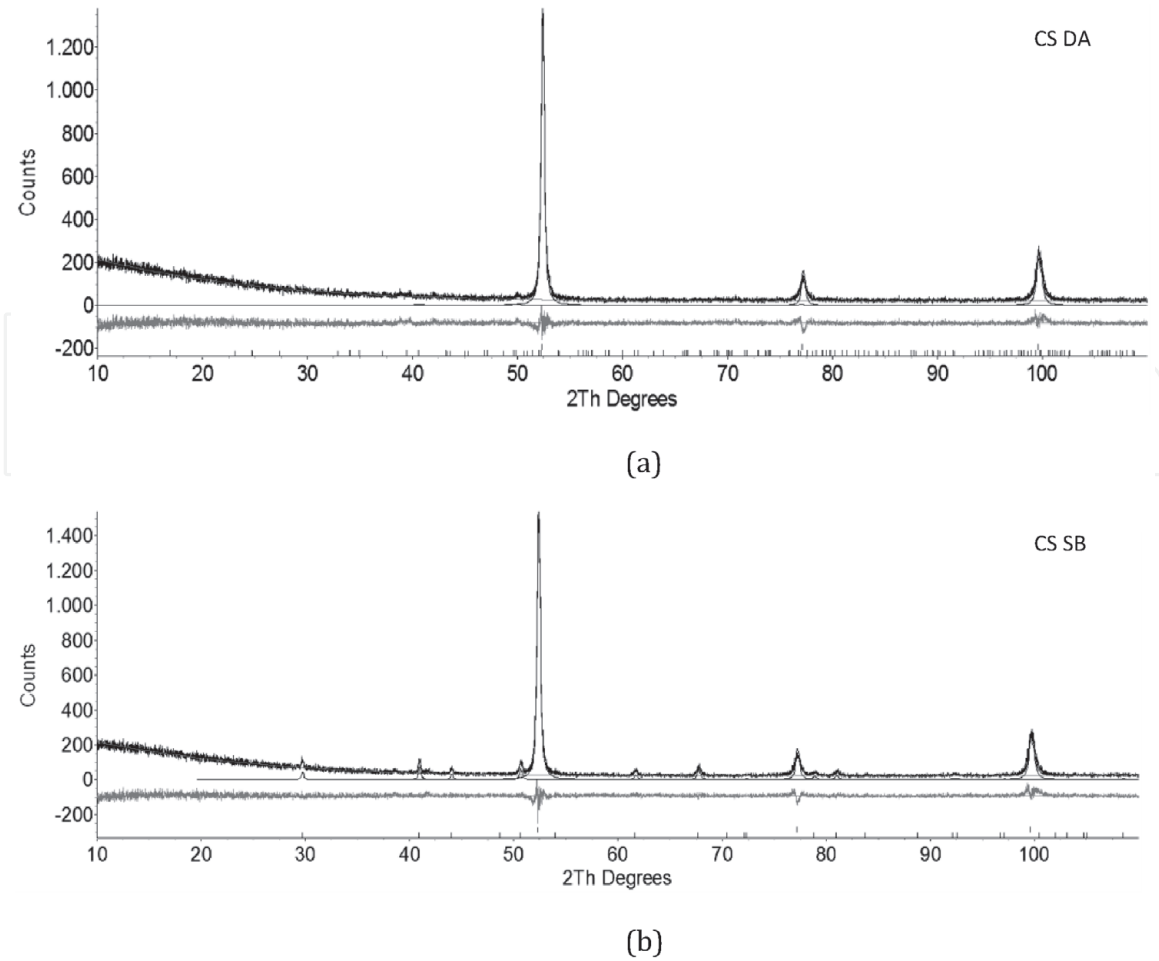


Figure 3. Carbon steel substrate blasted with (a) DA and (b) SB abrasives. Observed data are indicated by thicker lines and calculated data by a solid thinner line. The gray lower curve presents the difference (residue) between the observed and calculated powder diffraction patterns.

Zero error (2θ) sample displacement, absorption ($1/\text{cm}$), and lattice parameters of the phases were not fixed to provide the best calculated fitting.

3.3.2 Fitting criteria

Fitting criteria is a way to analyze the accuracy and precision of fitting. Based on the R-weighted pattern (R_{wp}) and the R-expected pattern (R_e), it is possible to calculate the “goodness of fit,” or simply *GOF*, to address the calculated values. Eqs. 4 and 5 present the variables used for the calculations for the R-values, which are then used to calculate the GOF [43–45]:

$$R_{wp} = \left[\left(\sum w_i (y_i(\text{obs}) - y_i(\text{calc}))^2 \right) / \left(\sum w_i (y_i(\text{obs})^2) \right) \right]^{1/2} \quad (4)$$

$$R_{exp} = \left[(N - P) / \left(\sum w_i (y_i(\text{obs})^2) \right) \right]^{1/2} \quad (5)$$

$$\text{GOF} = [(S_y) / (N - P)]^{1/2} = R_{wp} / R_{exp} \quad (6)$$

where y_i = intensity at the i th step; w_i = weighting factor; N = number of observations; P = number of parameters; obs = observed and calc = calculated.

Table 1 presents the GOF values for each calculation. The calculated values lied between 1 and 1.5, which is an indication of a satisfactory fitting. Numbers greater than 1.5 are usually seen as an inadequate model or false minimum, whereas those

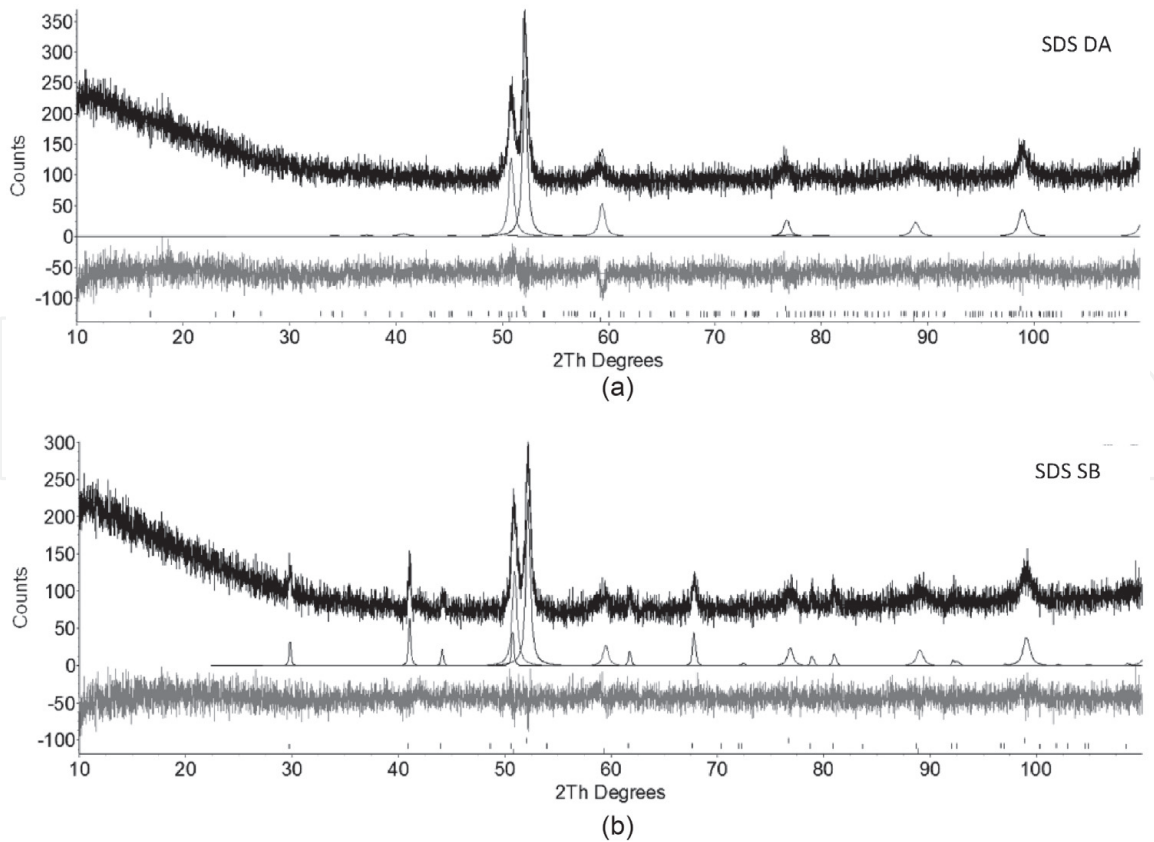


Figure 4.
 Super duplex steel substrate blasted with (a) DA and (b) SB abrasives.

Abrasive	CS substrate	SDS substrate
SB	1.14 ± 0.008	1.05 ± 0.007
DA	1.13 ± 0.010	1.07 ± 0.010
MCS	1.09 ± 0.012	1.06 ± 0.010
MSS	1.09 ± 0.011	1.06 ± 0.011

Table 1.
 Fitting criteria for Rietveld calculations: calculated average goodness of fitness for the set of four samples of each substrate per abrasive.

	% α-Fe	% γ-Fe	%Al ₂ O ₃
SB abrasive			
Super duplex	38.79 ± 1.84	25.01 ± 2.13	36.20 ± 2.92
Carbon steel	79.79 ± 2.37	*	20.21 ± 2.37
DA abrasive			
Super duplex	47.31 ± 2.21	36.92 ± 1.16	15.77 ± 2.52
Carbon steel	89.56 ± 0.59	*	10.45 ± 0.59

Table 2.
 Quantitative phase calculations results (calculated average and standard deviation for a set of four blasted samples).

lower than 1.0 show a model that contain more parameters than can be justified by the quality of the data, as insufficient counting time for processing or high influence of background, for example.

Table 2 presents the quantitative phase analysis results for abrasive contamination in both CS and DSS substrates. 36.20% of the SDS and 20.21% of the carbon steel blasted area were contaminated by SB particles. When analyzing the DA abrasive, 15.77% of the SDS area was contaminated, while 10.45% of the CS substrate depicted particle contamination. The higher percentage of contamination on the SDS substrate can be related with its high values of hardness. The consequences of such higher particle contamination, for the performance of anticorrosive organic coatings, can be found in a subsequent work [46].

4. Case 2: ferrite/austenite (α/γ) ratio in duplex steels and the occurrence of sigma phase: quantification of unbalanced phase formation and precipitation due to thermal treatments on the steel

Super duplex stainless steel (SDSS) is a class of steels that retain two equal balanced main phases within their microstructure, BCC α -Fe (ferrite) and FCC γ -Fe (austenite). In that manner, this material can combine good mechanical properties with high corrosion resistance. However, when subjected to welding or to high-temperature applications, thermal-activated diffusion mechanisms promote the precipitation of some deleterious phases in the SDSS matrix in addition to creating an unbalanced volume of ferrite and austenite. The unequal proportions of ferrite/austenite and the occurrence of phases such as sigma phase (also known as σ phase) can highly compromise the ability of these steels to support loads and to avoid corrosion, leading to higher rates of degradation. Therefore, it is mandatory that investigations on thermal cycles are carried on determining the critical time/temperature values that lead to this kind of phase unbalance.

Previous studies in different classes of duplex steels [47] have identified the temperature range of 300–1000°C as a critical range for phase transformations. Therefore, a series of heat treatments, involving different temperature ranges and time intervals, were performed in a UNS S32750 to study the phase formation in this specific class of duplex steel and to determine the amounts of ferrite, austenite, and sigma phase formed after each treatment. For this specific calculation, X-ray diffraction was displayed as a crucial tool for precise phase quantification in a specific volume of material. After all the samples were scanned, phase amounts were calculated using quantitative phase analysis by Rietveld refinement. These calculations lead to further experimental investigations using nondestructive evaluation techniques [48].

4.1 Heat treatments for different amounts of phase formation

Samples were cut as 70 mm \times 40 mm \times 6 mm steel plates. All samples were submitted to a preliminary solution heat treatment in order to obtain a balance of approximately 50% of α and γ phases. Then, aging treatments were performed to create the α/γ unbalance and the precipitation of sigma phase. **Figure 5** shows a schematic of the heat treatment steps.

The solution heat treatment was conducted as follows:

1. Three samples remained in the as-received condition, i.e., without any heat treatment for further comparison with the heat-treated samples.
2. The remaining samples were subjected to a solubilization treatment, which consists of heating up to 1220°C for 1 h, followed by water quenching.

3. Three of the solubilized samples did not receive any additional aging heat treatment and remained in the solubilized condition.
4. Then, a group of 14 samples received an additional aging heat treatment to introduced different fractions of sigma phase. The aging heat treatment was conducted at 1000°C for different time intervals, followed by water quenching.
5. Finally, seven samples were heat treated at 1320 and at 1350°C for different intervals, in order to have high amounts of delta phase but no sigma phase at all.

4.2 X-ray analysis results

Phase volumetric fractions were measured in nine different regions of each sample, as depicted in **Figure 6**. Diffraction parameters used were the same presented in item 3.2 from this chapter.

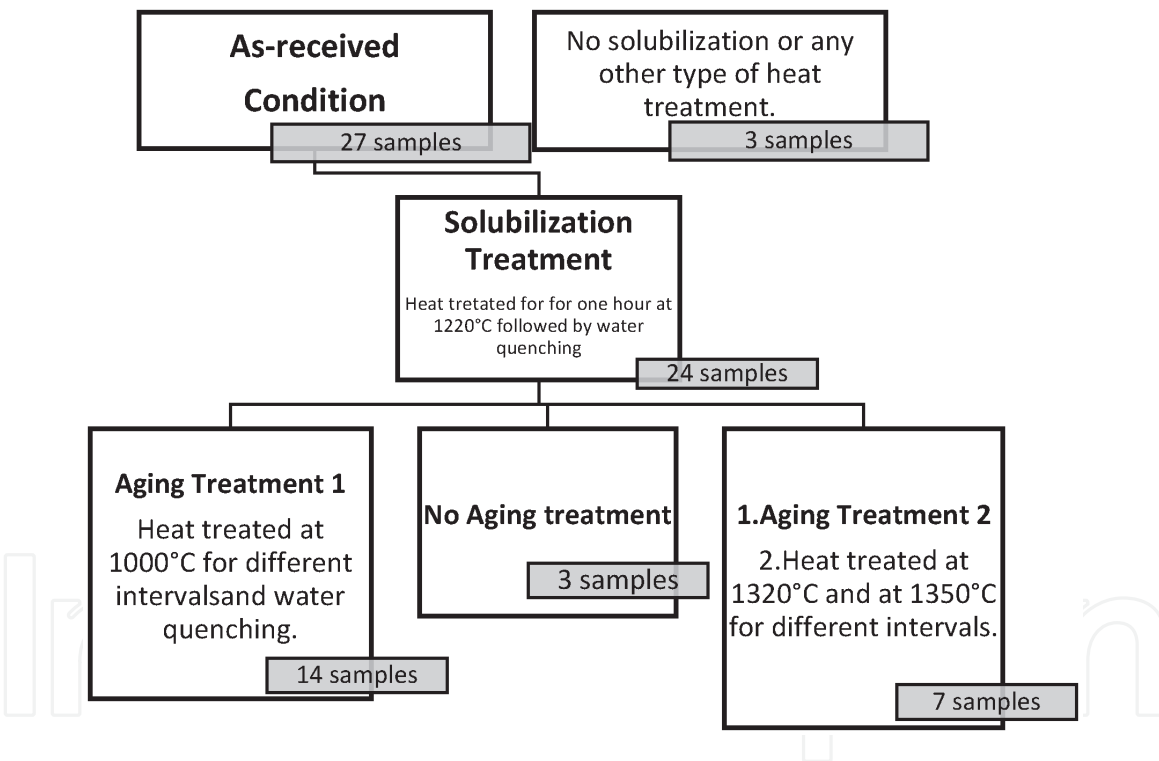


Figure 5.
 Schematics of heat treatments performed in the SDSS samples.

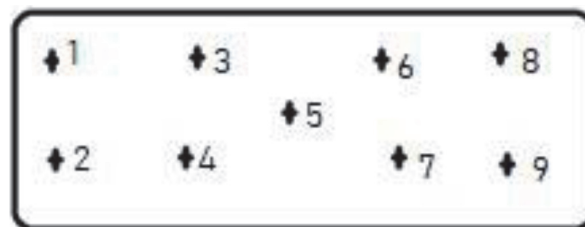


Figure 6.
 Schematics of a sample with its nine analyzed points.

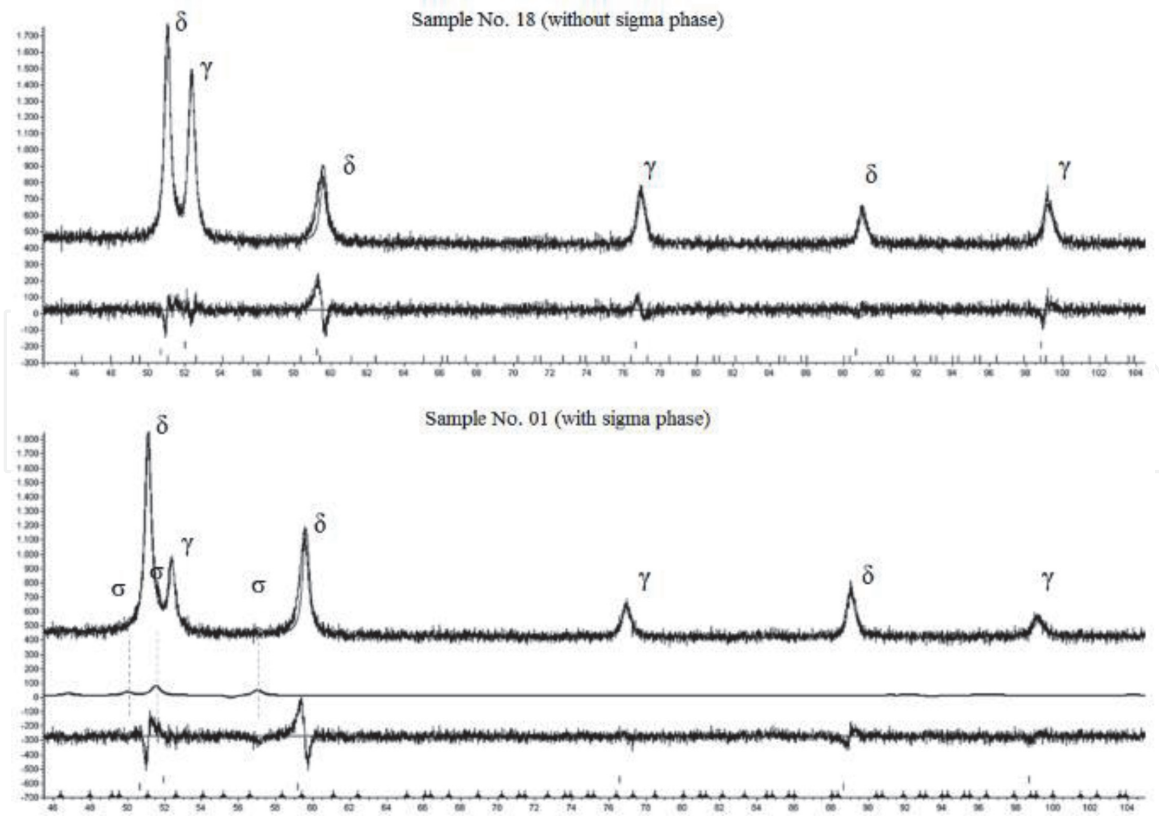


Figure 7.
XRD spectrum for two different conditions. Sample number 18 without σ phase and sample number 01 with 3.4% of σ phase.

Samples	Temperature ($^{\circ}\text{C}$)	Time (min)	γ phase (%)	α phase (%)	σ phase (%)
01	1000	60	64.0 ± 2.3	32.5 ± 2.7	3.4 ± 1.0
02	1000	45	49.3 ± 3.0	47.5 ± 3.5	3.1 ± 0.9
03	1000	22	64.3 ± 3.9	32.6 ± 4.0	3.0 ± 0.6
04	1000	45	62.4 ± 4.3	34.8 ± 4.1	2.7 ± 0.7
05	1000	25	52.2 ± 12.1	45.1 ± 11.5	2.6 ± 1.2
06	1000	25	65.1 ± 9.8	31.7 ± 7.8	2.4 ± 1.1
07	1000	5	68.1 ± 7.9	29.6 ± 8.2	2.2 ± 0.7
08	1000	60	61.1 ± 5.0	36.6 ± 4.9	2.1 ± 1.9
09	1000	20	64.4 ± 4.5	33.4 ± 4.5	2.1 ± 0.2
10	1000	20	56.7 ± 6.5	41.2 ± 6.9	2.0 ± 0.7
11	1000	1	57.9 ± 5.5	40.4 ± 5.3	1.6 ± 0.6
12	1000	1	59.3 ± 7.1	39.0 ± 7.1	1.6 ± 0.2
13	1000	6	68.5 ± 3.6	29.9 ± 3.6	1.5 ± 0.4
14	1000	10	61.6 ± 5.4	37.0 ± 5.3	1.2 ± 0.4
15	As received		47.7 ± 2.0	52.2 ± 2.0	0.0
16	As received		44.2 ± 4.9	55.7 ± 4.9	0.0
17	As received		47.1 ± 1.6	52.8 ± 1.6	0.0
18	1220	60	50.2 ± 7.8	49.7 ± 7.7	0.0
19	1220	60	56.8 ± 5.1	43.1 ± 5.1	0.0
20	1220	60	54.3 ± 5.7	45.7 ± 5.7	0.0

Samples	Temperature (°C)	Time (min)	γ phase (%)	α phase (%)	σ phase (%)
21	1320	60	38.8 ± 3.3	61.1 ± 2.9	0.0
22	1320	60	28.3 ± 5.1	71.6 ± 5.0	0.0
23	1320	120	44.8 ± 3.0	55.1 ± 3.0	0.0
24	1320	60	36.2 ± 7.4	63.7 ± 7.4	0.0
25	1320	240	41.7 ± 6.9	58.2 ± 6.9	0.0
26	1350	60	34.4 ± 6.4	65.7 ± 6.3	0.0
27	1350	60	40.5 ± 8.7	59.4 ± 8.6	0.0

Table 3.
 Phase volume contents according to heat treatment temperatures and time intervals.

4.2.1 Fitting parameters

The structure refinement used the fifth-degree Chebyshev polynomial [38] to fit the background intensities, y_{ib} , (according to Eq. 2), as well as the 1/x background function, from Topas 4.2. α -Fe and γ -Fe and sigma phases were fitted to the preferred orientation March-Dollase model [39–41].

4.2.2 Fitting criteria

The fitting criteria followed the same methodology applied in Case 1, using Eqs. (4)–(6). For every sample, the GOF was within the range of 1.0–1.5.

4.2.3 Phase calculations

Figure 7 depicts two diffractograms—one from a sample containing only ferrite and austenite and another containing both phases and sigma. QPA (using Rietveld refinement) was carried on each one of the nine described points for each sample, generating similar scans to the ones presented in **Figure 7**. Each scan was then carefully analyzed and adjusted accordingly to the chosen fitting parameters to assure a GOF between 1.0 and 1.5, i.e., the best fit possible.

The values obtained for each point were then summed and averaged and the standard deviation calculated for each sample average. **Table 3** presents those calculated values.

5. Conclusions

X-ray diffraction has demonstrated to be an effective tool for phase analysis in metallic materials, especially in steels. Because this type of material is the most used material on earth nowadays, due to its versatility in terms of physical, mechanical, and chemical properties, knowledge of the phase transformations that might occur during service and processing is ultimate.

Steel surfaces subjected to abrasive surface cleaning, which suffered contamination from the blasting operation, and duplex steels subjected to aggressive environments and high temperatures of service, which experienced phase transformation, were analyzed by X-ray diffraction using peak refinement, by the Rietveld method.

The refinement method demonstrated that phase identification and quantification enabled the diagnosis of forthcoming problems related to the presence of such

phases in the investigated steels, allowing the optimization of techniques and the choice of correct process parameters.

Acknowledgements

The authors would like to acknowledge the staff and professors from the Laboratório de Ensaios Não Destrutivos Corrosão e Soldagem (LNDC, Rio de Janeiro, Brazil) that were fundamental for the realization of this work, as well as the Department of Materials Sciences and Metallurgy (DMM) of the Federal University of Rio de Janeiro (UFRJ).

Conflict of interest

The authors declare no conflict of interest.

Thanks

The authors would like to thank professor Isabel Margarit-Mattos for the opportunity of developing this investigation on the blasted steel surfaces from her research on organic coatings.

Author details

Adriana da Cunha Rocha* and Gabriela Ribeiro Pereira
Federal University of Rio de Janeiro (UFRJ), Rio de Janeiro, Brazil

*Address all correspondence to: adrirocha@metalmat.ufrj

IntechOpen

© 2020 The Author(s). Licensee IntechOpen. This chapter is distributed under the terms of the Creative Commons Attribution License (<http://creativecommons.org/licenses/by/3.0>), which permits unrestricted use, distribution, and reproduction in any medium, provided the original work is properly cited. 

References

- [1] Armas IA, Moreuil SD. Duplex Stainless Steels. New Jersey: Wiley; 2009
- [2] Bernhardsson S, Oredsson J, Martenson C. Duplex Stainless Steels. Metals Park, Ohio, USA: ASM International; 1983
- [3] Porter DA, Easterling KE. Phase Transformations in Metals and Alloys. 2nd ed. United States: Springer; 1992
- [4] ASM International Handbook Committee. ASM Handbook, Vol. 1: Properties and Selection: Irons, Steels, and High-Performance Alloys. Novelty, OH, USA: ASM International; 2009
- [5] Cullity BD. Elements of X-Ray Diffraction. 2nd ed. Boston: Addison-Wesley Publishing Company; 1978
- [6] Rietveld HM. A profile refinement method for nuclear and magnetic structures. Journal of Applied Crystallography. 1969;2(2): 65-71
- [7] Young R. The Rietveld Method. New York: Oxford University Press; 1995
- [8] Hill RJ, Howard CJ. Quantitative phase analysis from neutron powder diffraction data using the Rietveld method. Journal of Applied Crystallography. 1987;20:467-474
- [9] Schweitzer PA. Corrosion Engineering Handbook. 2nd ed. Florida: CRC Press; 2007
- [10] Satas D, Tracton AA. Coatings Technology Handbook. 3rd ed. Florida: CRC Press; 2005
- [11] Momber A. Blasting Cleaning Technology. Berlin: Springer; 2008
- [12] Momber A, Wong YC. Overblasting effects on surface properties of low-carbon steel. Journal of Coating Technology and Research. 2005;2(6): 453-461
- [13] ISO 4628-2. Paints and Varnishes, Evaluation of Degradation of Coatings—Designation of Quantity and Size of Defects and of Intensity of Uniform Changes in Appearance—Assessment of Degree of Blistering. Switzerland: International Organization for Standardization; 2003
- [14] ISO 8501-1. Preparation of Steel Substrates before Application of Paints and Related Products. Visual Assessment of Surface Cleanliness. Rust Grades and Preparation Grades of Uncoated Steel Substrates and of Steel Substrates After Overall Removal of Previous Coatings. Switzerland: International Organization for Standardization; 2007
- [15] Morcillo M, Bastidas M, Simancas J, Galvan JC. The effect of the abrasive work mix on paint performance over blasted steel. Anti-Corrosion Methods and Materials. 1989;36(5):4-8
- [16] ASTM E1245-03. Practice for Determining the Inclusion or Second-Phase Constituent Content of Metals by Automatic Image Analysis. USA: American Society for Testing and Materials, ASTM International; 2003
- [17] Zevin LS, Kimmel G. Quantitative X-Ray Diffractometry. Berlin: Springer; 1995
- [18] Klug HP, Alexander LE. X-Ray Diffraction Procedures for Polycrystalline and Amorphous Materials. 2nd ed. New Jersey: John Wiley & Sons; 1974
- [19] Hubbard CR, Snyder RL. RIR—Measurement and use in quantitative XRD. Powder Diffraction. 1988;3(2): 74-77

- [20] Chung FH. Quantitative interpretation of X-ray diffraction patterns of mixtures. I. Matrix-flushing method for quantitative multicomponent analysis. *Journal of Applied Crystallography*. 1974;7:519-525
- [21] Bish DL, Howard SA. Quantitative phase analysis using the Rietveld method. *Journal of Applied Crystallography*. 1988;21:86-91
- [22] Bish DL, Chipera SJ. Problems and solutions in quantitative analysis of complex mixtures by X-ray powder diffraction. *Advances in X-Ray Analysis*. 1987;31:295-308
- [23] Bish DL, Chipera SJ. Accuracy in quantitative X-ray powder diffraction analyses. *Advances in X-Ray Analysis*. 1995;38:47-57
- [24] Chipera SJ, Bish DL. Multireflection RIR and intensity normalizations for quantitative analyses: Applications to feldspars and zeolites. *Powder Diffraction*. 1995;10(1):47-55
- [25] Snyder RL, Bish DL. Quantitative analysis—Modern powder diffraction. In: Bish DL, Post JE, editors. *Reviews in Mineralogy*. Vol. 20. Denver: Mineralogical Society of America; 1989. pp. 101-144
- [26] Sidey V. A simplified correction function for the effect of surface roughness in X-ray powder diffraction. *Journal of Applied Crystallography*. 2004;37:1013-1014
- [27] Paiva-Santos CO, Marques RFC, Franco MK, Silva MT, Jafelicci-Jr M. Surface Roughness Effect on the B's Values in the Rietveld Refinement. 2002. Available from: <http://labcacc.iq.unesp.br/publicacoes/sr/sreffect.htm>
- [28] Sparks CJ, Kumar R, Specht ED, Zschack P, Ice GE, Shiraishi T, et al. Effect of powder sample granularity on fluorescent intensity and on thermal parameters in X-ray diffraction Rietveld analysis. *Advances in X-Ray Analysis*. 1992;35:57-62
- [29] Pitschke W, Hermann H, Mattern N. The influence of surface roughness on diffracted X-ray intensities in Bragg-Brentano geometry and its effect on the structure determination by means of Rietveld analysis. *Powder Diffraction*. 1993;8(2):74-83
- [30] Pitschke W, Mattern N, Hermann H. Incorporation of microabsorption corrections into Rietveld analysis. *Powder Diffraction*. 1993;8(4):223-228
- [31] Suortti P. Effects of porosity and surface roughness on the X-ray intensity reflected from a powder specimen. *Journal of Applied Crystallography*. 1972;5:325-331
- [32] Bruker AXS. *Topas: General Profile and Structure Analysis Software for Powder Diffraction Data*. Karlsruhe: GmbH; 2003
- [33] Cheary RW, Coelho A. A fundamental parameters approach to X-ray line-profile fitting. *Journal of Applied Crystallography*. 1992;25(2):109-121
- [34] Gorton AT, Bitsianes G, Joseph TL. Thermal expansion coefficients for iron and its oxides from X-ray diffraction measurements at elevated temperatures. *Transactions of the Metallurgical Society of AIME*. 1965;233(8):1519-1525
- [35] Ridley N, Stuart H. Partial molar volumes from high-temperature lattice parameters of iron-carbon austenites metal. *Science Journal*. 1970;4:219-222
- [36] Morris MC et al. Standard X-ray diffraction powder patterns. National Bureau of Standards (U.S.), Circ 539. 1960;9:3

- [37] Olivier B, Retoux R, Lacorre P, Massiot D, Ferey G. Crystal structure of κ -alumina: An X-ray powder diffraction, TEM and NMR study. *Journal of Materials Chemistry*. 1997;7:1049
- [38] Boyd JP. Chebyshev and Fourier Spectral Methods. 2nd ed. New York: Dover Publications; 2001
- [39] March A. Mathematische Theorie der Regelung nach der Korngestalt bei affiner Deformation. *Zeitschrift fuer Kristallographie*. 1932;81:285-297
- [40] Dollase WA. Correction of intensities for preferred orientation in powder diffractometry: Application of the March model. *Journal of Applied Crystallography*. 1986;19:267-272
- [41] Zolotoyabko E. Determination of the degree of preferred orientation within the March-Dollase approach. *Journal of Applied Crystallography*. 2009;42:513-518
- [42] Solomentsev ED. In: Hazewinkel M, editor. *Encyclopedia of Mathematics*. Berlin: Springer; 2001
- [43] E. Prince E. In: Wilson AJC, editor. *Structure and Statistics in Crystallography*. New York; 1985. pp. 95-108
- [44] Young RA, Wiles DB. Profile shape functions in Rietveld refinements. *Journal of Applied Crystallography*. 1982;15:430-438
- [45] Young RA, Prince E, Sparks RA. Suggested guidelines for the publication of Rietveld analyses and pattern decomposition studies. *Journal of Applied Crystallography*. 1982;15: 357-359
- [46] Nascimento AV. Aspects of surface treatments of super duplex stainless steels for application of anticorrosive coatings [Thesis]. Rio de Janeiro, Brazil: UFRJ; 2009
- [47] Yamashita M, Matsumoto S, Hironata N. Corrosion resistance and properties of duplex stainless steels. In: *International Conference & Expo Duplex Stainless Steels'07*; Italy, June. 2007
- [48] Camerini C, Sacramento R, Areiza MC, Rocha A, Santos R, Rebello JM, et al. Eddy current techniques for super duplex stainless steel characterization. *Journal of Magnetism and Magnetic Materials*. 2015;388:96-100